

A simulation Study for Assessing the Impact of Fast Reserve with Additional Synthetic Inertia Control on the Continental Europe Synchronous Area

Fabio Massaro ¹, Rossano Musca ¹, Antony Vasile^{1, *} and Gaetano Zizzo ¹

¹ Department of Engineering, Università degli Studi di Palermo, 90128, Italy;
fabio.massaro@unipa.it; rossano.musca@unipa.it; antony.vasile@unipa.it; gaetano.zizzo@unipa.it

* Correspondence: antony.vasile@unipa.it; Tel: +39 328-772-6725

Abstract

This article shows the results of a simulation study on the application of battery storage systems in Fast Reserve Unit (FRU) configuration with an additional control for providing synthetic inertia. The base hypothesis of the study is to assess the impact of the extension of the regulation provided by the FRUs to all the Continental Europe Synchronous grid with the same power proportions of the first Italian FRU auction. The simulations are conducted in two different scenarios: a base one related to 2020 and a future one related to 2040 and based on ENTSO-E projections for load and generation. The results show that, for the reference incident of 3000 MW, the frequency quality parameters in 2040 are significantly worse than those in 2020 but, with the injection of the FRUs with additional synthetic inertia control, there is an improvement both in dynamic and steady-state. The study shows how 2040 frequency parameters can become comparable with the current ones if minimum shares of fast reserve and synthetic inertia are provided to improve the stability of the grid. Finally, starting from the incident occurred the 8th of January 2021, it is shown by simulations how FRUs can support the grid also during a system split.

Keywords: synthetic inertia; storage; Fast Reserve Unit; primary regulation; Continental Europe.

1. Introduction

The energy transition towards sustainable sources is reducing the presence in the European generating system of traditional fuel-based plants in favor of renewable sources. While this transformation, on the one hand, has undeniable environmental advantages, it nevertheless poses some critical issues due to the uncertainty and intermittency of these sources, and to the significant reduction in the inertia of the system and the frequency containment reserve [1-3]. The documents recently published by ENTSO-E [4] highlight that the European electric power system needs some actions such as the development of new interconnections, the increase of the storage capacity, and new auxiliary

services (e.g. fast frequency regulation and synthetic inertia (SI)) [4-6]. Fast or ultra-rapid frequency regulation, in particular, is one of the new ancillary services that seems to have become indispensable due to the changes that have occurred in the electricity system in recent years. In 2019, Terna, the Italian transmission system operator (TSO), launched a pilot project called Fast Reserve Units (FRU), to address the reduction in the frequency regulation response due to the decrease in traditional fossil fuels [7]. An FRU, thanks to the implementation of appropriate control logics, can guarantee adequate responses to a disturbance (e.g. frequency deviation), contributing to keeping the power supply system stable during a power imbalance. If suitably controlled, the same units can be used also for providing synthetic inertia [4], contributing to the RoCoF containment in the first moments of a disturbance. In this work, after having listed the main requirements for the Italian FRU service qualification and having presented the models implemented for simulating the fast reserve and synthetic inertia services, the presence of FRUs connected to the Continental Europe (CE) Synchronous grid is simulated in Matlab/Simulink in two different scenarios: a base one related to 2020 and a future one related to 2040 and based on ENTSO-E projections for load and generation. The novelty of the study is in presenting the impact of a large adoption of FRUs in the CE synchronous area and in considering the possibility of integrating their action with SI control. Previous study dealt with fast frequency regulation and SI in the European power grid. In [8], the authors presented a review on fast frequency control services implemented in Europe, focusing on their remuneration. In [9], the authors assessed the impact of frequency variations in UK and CE areas on the aging of batteries providing enhanced frequency control. Finally, in [10], the authors presented the idea of wind inertial response based on the center of inertia of a control area, testing their proposal on the interconnected power system of the Southern-Eastern Europe.

One of the strong points of the present analysis, with respect to these previous works, it is in the modeling of the CE area, based on ENTSO-E Initial Dynamic Model [11] and energy projections, that provides a realistic dynamic behavior of the European power system. Moreover, two criteria for a possible distribution of the FRUs among the CE area countries are proposed. Finally, the paper provides also a simulation analysis showing how the action of FRUs dislocated on the whole CE synchronous area could have improved the frequency transient during the system split occurred on the 8th of January 2021.

2. Fast Reserve Unit

On November 20, 2019, Terna issued a document for public consultation related to a pilot project for the provision of ultra-fast frequency regulation service called “Fast Reserve”. The ultra-rapid frequency regulation service is one of the answers to the new needs imposed by the evolution of the

electric power system. The service provided by Fast Reserve Unit responds to the progressive reduction of the response time of the primary frequency regulation due to the carbon phase-out [12-13]. This grid service will contribute to improving the stability of the grid frequency, in coordination with existing grid services such as primary reserve.

The consultation ended on January 24, 2020 while the approval of the regulation took place on June 3, 2020 with resolution 200/2020/R/eel by ARERA [14]. Following approval by the Authority, FAQs were published in September and November, and a document containing estimated hours of availability for the year 2021 was published on November 6, 2020 [15]. The auction for the allocation of available capacity was held on December 10, 2020. The available qualified power was 230 MW to be distributed throughout the country. The auction registered good participation: 53 operators, 117 Fast Reserve Units for a total qualified power value of about 1,327.3 MW, over six times the available qualified power [16]. Table 1 reports in detail the timeline of the FRU project. There are 17 assigned operators with a total of 23 plants: in addition to Terna's interest in creating a new flexibility service based on storage systems, this participation demonstrates the great interest of grid operators in this new regulatory service.

Technically, the definition of an FRU is given by Article 2.1 of the regulations [13]: *“Fast Reserve Units are individual devices connected directly or indirectly to the public network or aggregates of devices that meet the technical requirements set out in Article 3 of the present regulation. Such devices may be:*

- (a) stand-alone generating units;*
- (b) generating units sharing the point of connection to the public grid with one or more consumption units other than ancillary services and/or storage facilities;*
- (c) consumption units, except for those units providing interruptibility service;*
- (d) storage plant, as defined according to ARERA Resolution 574/2014, both "stand-alone" and combined with generation units and/or consumption units.”*

The main requirement for the qualification of the plant to the FRU service are:

- qualified Power P_q (i.e., the power available for regulation) within the range 5-25 MW;
- provide a continuous and automatic power response proportional to the disturbance and therefore to the frequency error as reported in the frequency-power regulation curve of Figure 1, activated without intentional delay and in any case within 1 second from the disturbance;
- if there are no further disturbances and therefore other frequency errors, it is necessary to maintain the power value continuously for at least 30 s and then reduce it over the next 5 minutes;
- be able to receive and manage the pilot set-point command sent by the TSO;

- be sized in such a way as to have sufficient energy capacity for a stable exchange with the electrical system with a power value at least equal to the Qualified Power, in injection or absorption, for at least 15 continuous minutes.

Table 1. Fast Reserve Unit Project timeline

Date	Event
20/11/2019	Opening consultation of the project
20/11/2019	Publication of the regulation and attachments
15/01/2020	Extension of consultation
15/01/2020	Fast Reserve Workshop
24/01/2020	Closing consultation
03/06/2020	Regulation approval (ARERA)
25/09/2020	FAQ Fast Reserve, I release
06/11/2020	FAQ Fast Reserve, II release
06/11/2020	Hour availability for 2021
10/12/2020	Auction for 2021

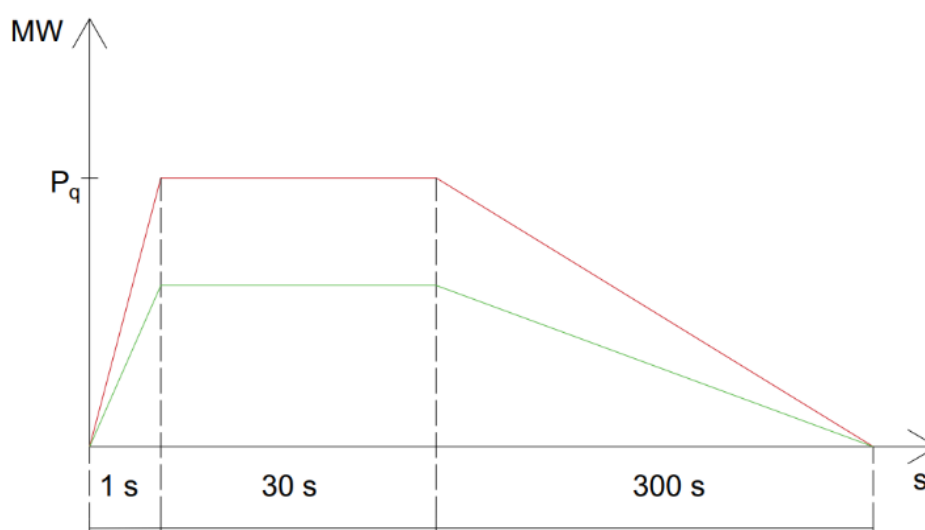


Figure 1. Regulation curve $\Delta P(t)$. The green curve is an example of service delivery for an event that does not require the full exploitation of the FRU potential; the red curve represents the upper limits of the ramping, constant and de-ramping phases. Source: Terna [13].

From the point of view of precision, two conditions must be respected:

- Dynamic accuracy: in case of frequency deviations sufficiently greater to activate the service, the power exchange must be within a defined area (Figure 2);

- Static accuracy: 1 second after the frequency deviation that caused the service activation, and in the absence of further changes, the actual power exchanged with the grid can be in a tolerance range of $\pm 1\%$ of the qualified power from the expected value.

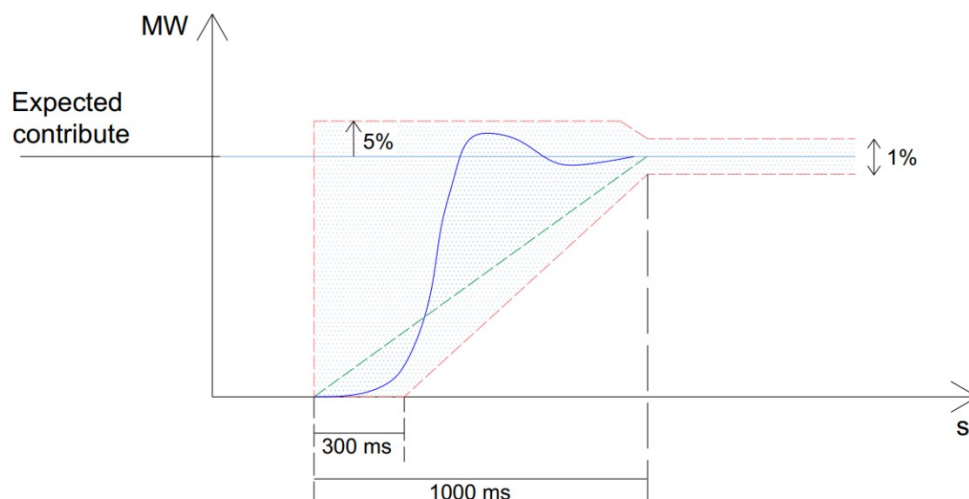


Figure 2. Static and dynamic accuracy curve, source Terna [13].

The requirements outlined above are only a part of the set of characteristics needed for the qualification of an FRU plant. The contribution provided by a FRU is comparable to that of primary regulation implemented by a static power converter that scientific literature identifies as rapid or improved frequency regulation [17-18]. Therefore, the production or consumption of power in the Point of Common Coupling (PCC) of the FRU is obtained through the implementation of a control scheme with a proportional regulator (Figure 3).

The technical specification for the Italian FRU indicates the following characteristics: an intentional dead band of first activation in the range 0-500 mHz (threshold # 1) and an additional threshold (threshold # 2 or saturation band) in the range threshold #1-1000 mHz, beyond which the consumed/produced power must be guaranteed as long as the frequency deviation exceeds the threshold and for the entire time allowed by the stored energy.

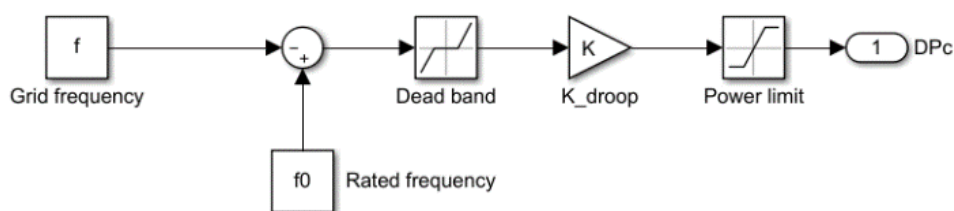


Figure 3. Implementation in Matlab/Simulink of the control scheme for fast frequency regulation.

In Figure 3:

- K_{droop} is the gain of the proportional regulator;
- DPc is the power variation at the PoC provided by the FRU system.

The correct operation of the system is guaranteed by the setting of the following parameters: the width of the dead band and of the saturation band, the gain of the regulator, and the qualified power of the device (represented by the positive and negative limits of the “Power limit” block shown in Figure 3). In this document, the parameters in Table 2 are assumed for simulations.

Table 2. FRU setting parameters.

Parameters	Values
Dead band f_{db}	50 Hz \pm 20 mHz
Saturation band f_{sat}	50 Hz \pm 500 mHz
Maximum power P_{MAX}	25 MW
Proportional gain K_{droop}	$K_{droop} = P_{MAX} / (f_{sat} - f_{db})$

3. Virtual Inertia Control

Although the recourse to renewable energy sources for power production leads to a reduction in polluting gas emissions, the penetration of renewable energy sources into the electric power system results in the weakening of the grid with a consequent increase in the risk of instability. The electrical machine responsible for generating power in the traditional system is the alternator. The rotating nature of the machine makes it react to any variation in the load in such a way as to counteract the variation itself and maintain, at least in the first moments, the electrical balance.

In an electrical system with rotating generators, an imbalance between load and generator leads to a frequency variation. This concept is presented in mathematical form by the *swing equation* [19-20]:

$$P_{gen} - P_{load} = J\omega_g \frac{d\omega_g}{dt}$$

where P_{gen} is the generated power, P_{load} is the load power (including losses), J is the inertia moment and ω_g is the generator angular speed [rad/s] (directly related to frequency). The inertia of a power system is defined as the ability of the system to resist frequency changes due to the kinetic energy

of the rotating masses. The power system's inertia constant H is the kinetic energy of the generators normalized to the apparent power S_g of all the generators connected to the system:

$$H = \frac{J\omega_g^2}{2S_g}$$

Performing the dimensional analysis, it can be seen that the inertia constant of the machine has the dimensions of a time. This can be interpreted as the *time for which the energy accumulated in the rotating masses can supply the load with a power equal to the apparent nominal power of the generator*.

Starting from the inertia of a single machine, it is possible to calculate the inertia of all the synchronous machines connected to the same grid as a weighted average of the inertia constants of all the generators, evaluated with respect to their rated power:

$$H_{syn} = \frac{\sum_{i=1}^n S_{gi}H_i}{S_{syn}}$$

where H_{syn} is the total system inertia, S_{gi} is the rated power of the i -th generator, H_i is the inertia of the i -th generator and S_{syn} is the total rated power of the system.

Substituting the expression of H_{syn} into the swing equation, it is obtained:

$$\frac{2H_{syn}}{f} \frac{df}{dt} = \frac{P_{gen} - P_{load}}{S_{syn}}$$

The term $\frac{df}{dt}$ is the Rate of Change of Frequency (RoCoF) of the system. The higher is the inertia constants of the generators, the higher will be the inertia of the system and the stronger it will be in case of serious disturbances and imbalances. Different generators have different inertia constant depending on the source of energy and conversion technology [21]. Renewable energy sources are connected to the grid via electronic converters with no rotating masses. It follows that the kinetic energy associated with them is zero, as well as the constant of inertia. To consider the effect of inverter-based generators, the system inertia H_{sys} can be reformulated as:

$$H_{sys} = \frac{\sum_{i=1}^n S_{gi}H_i}{P_{load}}$$

where P_{load} is the power requested by the load [21].

With a high penetration of inverter-based sources, the global system inertia drops and, as a consequence of this, the system is more affected by power imbalances with issues on stability and reliability.

The same converters of RES plants can provide an important contribution to the system inertia: if correctly controlled, a converter can provide a response similar to that of an alternator: this “virtual” regulation is defined as *Synthetic Inertia* (it can often be referred also as *artificial*, *emulated*, or *virtual*). In the literature, there are several SI topologies [22], each one different from another for mathematical models, control algorithms, performances, and applications. Figure 4 shows a classification of the different topologies. For this paper's purposes, the authors use the method proposed in [23].

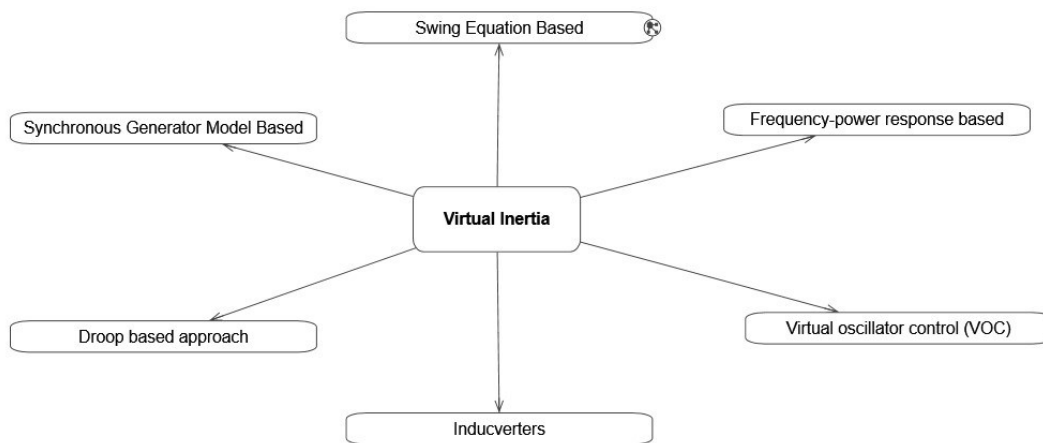


Figure 4. Classification of different topologies of Virtual Inertia control schemes.

With reference to the previous classification [22], the control scheme proposed in [23] belongs to the “frequency-power response based” models, as it performs a constant control on the network frequency to calculate the power contribution to be delivered. The chosen method is characterized by a straightforward implementation that fits the scope of this paper, which is to show the potential of an extension of FRU implementation of the whole CE area, and it is the modeling approach usually adopted for this category of analyses, since it well represents the dynamic of a complex system. As an example, in [24] it has been applied to the Sardinia power system. Other more accurate methods are not useful for such a preliminary assessment and, at the same time, some of them are not applicable to the FRU case since FRUs are operated as current source converters. Figure 5 shows the model implemented in Matlab/Simulink environment for simulating the SI control.

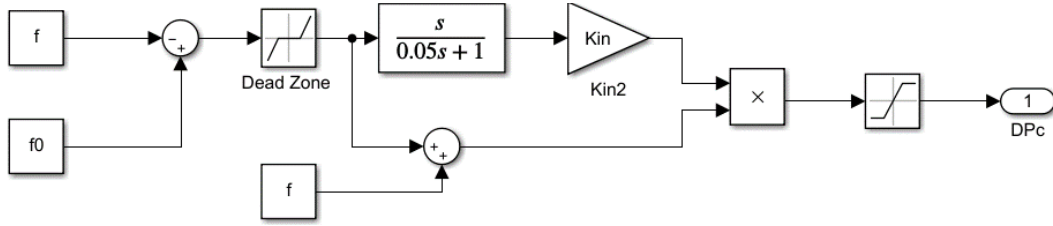


Figure 5. Implementation in Matlab/Simulink of the model for SI.

The value of the dead zone is the same imposed for the FRU (Table 1); the band is necessary to guarantee insensitivity in the event of small errors of the frequency. The derivative of the frequency deviation is calculated and subsequently multiplied by the instantaneous frequency value and by the gain of the controller K_{in} . This parameter is selected in relation to the RoCoF value assumed as acceptable [25]. The power consumed/produced for the SI service can be, therefore, written as it follows:

$$DP_i = K_{in} \cdot f \cdot df/dt$$

where DP_i is the power variation at the PoC provided by the converter due to the SI Control.

4. Simulations of Continental Europe Synchronous Areas with FRU and SI

4.1. Current Base Scenario 2020 and Future Base Scenario 2040, Traditional Primary Regulation

The starting point of the study is the dynamic simulation of CE grid for the Reference Incident, assumed 3000 MW, with the only support of the traditional primary regulation. The data of the system are extracted from the Initial Dynamic Model provided by ENTSO-E [11, 26], which has already been used in several works for the study of the primary frequency control in the CE synchronous area [27-30]. The penetration of renewable energy sources in the electrical system causes a decrease of both the inertia and the regulating energy of the system. The aim of the simulations is to evaluate the frequency dynamics with the RES share foreseen for 2040 by ENTSO-E [31-33], in the case of the same value of the Reference Incident. Figure 6 shows the model of the system implemented in Matlab/Simulink environment while Table 3 reports all data used in the simulations. The data related to the 2040 scenario are assessed by the authors starting from ENTSO-E projections [31-33].

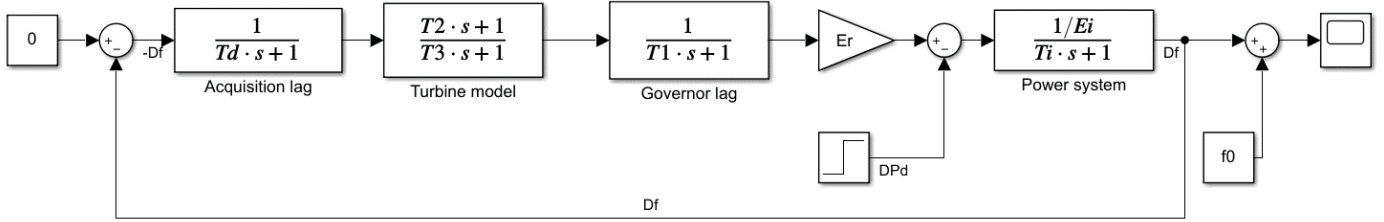


Figure 6. Implementation in Matlab/Simulink of the traditional primary regulation control.

The variables that characterize the scheme are, in order:

- T_1, T_2, T_3, T_d : power plants time constants (s);
- E_r : generators power-frequency characteristic (MW/Hz);
- DP_d : disturbance (MW);
- E_i : loads power-frequency characteristic (MW/Hz);
- T_i : time constant of the system (s);
- Df : frequency error (Hz);
- f_0 : nominal frequency (Hz).

Table 3. Data for the simulations of the current and future base scenarios.

Parameters	Base Scenario 2020	Base Scenario 2040
Initial load P_0	317000 MW	363000 MW
Initial Frequency f_0	50 Hz	50 Hz
Rated apparent power of the generators in the area A_n	462450 MVA	167500 MVA
System inertia H_s	3.71 s	1.71 s
Load regulating factor D	0.01	0.01
Load power frequency characteristic E_i	3170 MW/Hz	3630 MW/Hz
Generators power frequency characteristic E_r	30830 MW/Hz	11167 MW/Hz
Time constant of the system T_i	21.65 s	6.84 s
Generators start time constant T_d	0.05 s	0.05 s
Governor time constant T_1	0.5 s	0.5 s
Turbine derivative time constant T_2	4 s	4 s
Turbine delay time constant T_3	9 s	9 s
Disturbance DP_D	3000 MW	3000 MW

Figure 7 shows the frequency dynamic in the 2020 Base Scenario: the frequency nadir is $f_{nad} = 49.87$ Hz and the steady-state frequency is $\Delta f_{stat} = 49.91$ Hz. Figure 8 shows the frequency dynamic

in the future Base Scenario instead: it can be seen that the parameters related to the frequency are slightly worse: the frequency nadir is $f_{nad} = 49.72$ Hz while the value at steady state is $\Delta f_{stat} = 49.79$ Hz. Even if this values may seem near to those at 2020, it has to be considered that the steady-state frequency is below 49.80 Hz, considered as a limit by ENTSO-E in the case of a disturbance equal to the Reference Incident.

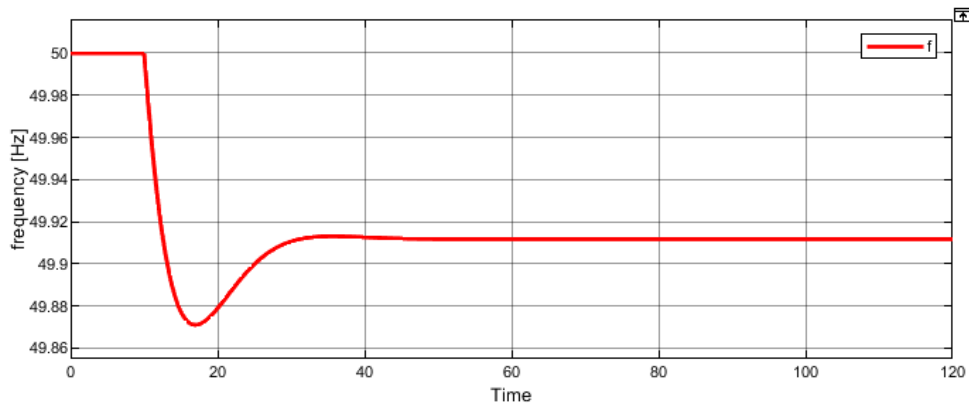


Figure 7. Frequency trend in the base scenario (2020).

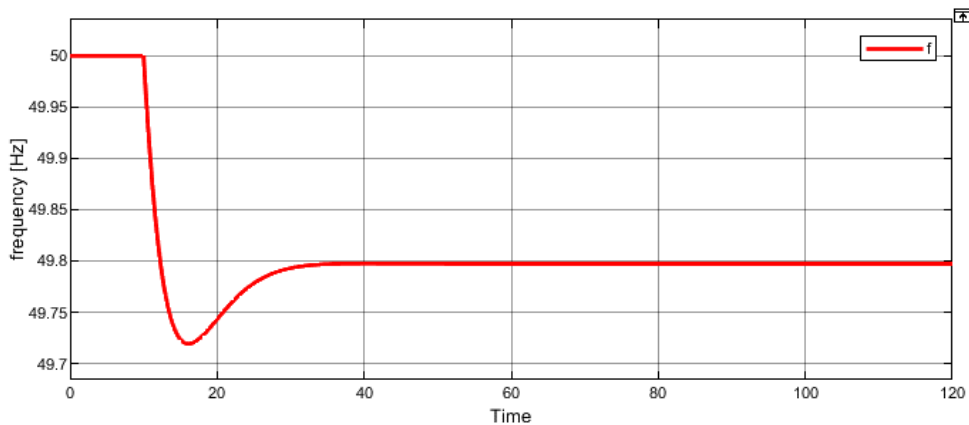


Figure 8. Frequency trend in the future scenario (2040) for the Reference Incident with traditional primary regulation.

After this first assessment considering only traditional primary regulation, in order to evaluate the contribution of the previously described technologies, two more simulations are presented in the following related to the 2040 scenario:

- Primary regulation with FRU support;
- Primary regulation with FRU support and additional SI control.

4.2. Primary regulation with Fast Reserve Unit in the 2040 Scenario

According to the control scheme shown in Figure 4, the FRUs were inserted in the traditional control scheme as shown in Figure 9. The input signal of the control is the same frequency deviation of the traditional control while the output is a power contribution DP_c that is added to the one provided by the rotating generators.

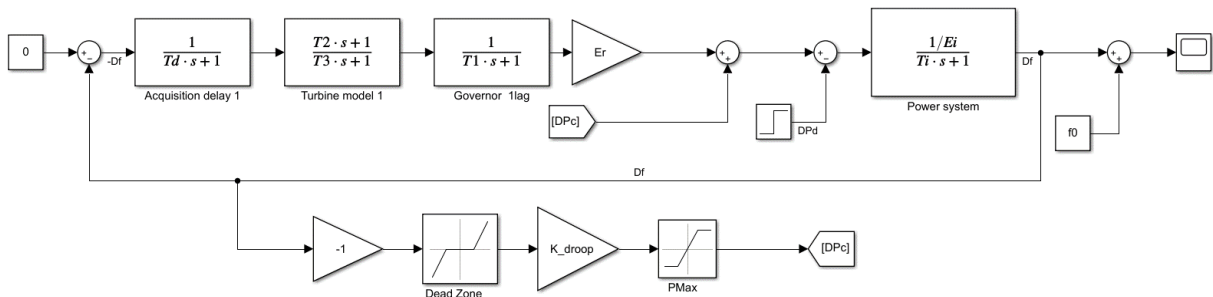


Figure 9. Implementation in Matlab/Simulink of the primary regulation control with FRUs.

The Qualified Power P_q of the FRUs was defined according to the same proportion used by Terna in the first auction of the pilot project: in order to compensate 6.6 GW of dismissed carbon power plants, the equivalent Qualified Power of the FRUs was established in 220 MW. According to the projections and following the same proportion, with the dismissal of 134 GW of fossil generation in 2040, the equivalent Qualified Power of FRU is 4060 MW. With regard to activation and saturation threshold, the first one is imposed to 20 mHz, while the second one is imposed to 1000 mHz. Table 4 summarizes the FRU setting parameters, while Figure 10 shows the frequency dynamics in this new scenario.

Table 4. FRU setting parameters.

Parameters	Values
Activation threshold	20 mHz
Saturation threshold	1000 mHz
Qualified Power P_Q	4060 MW

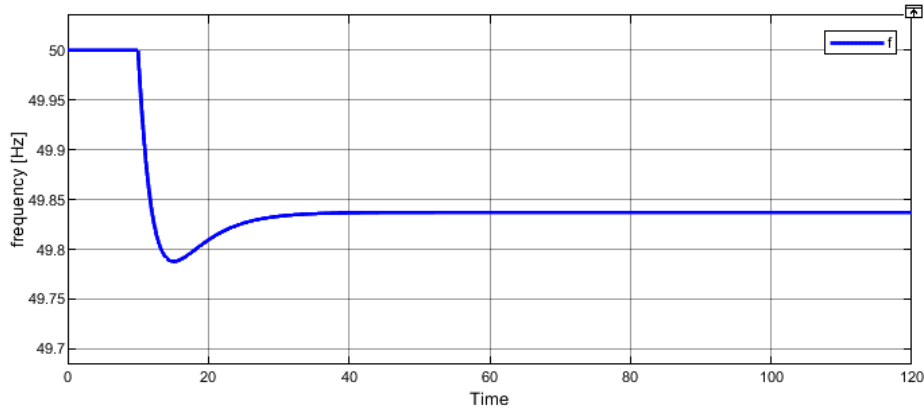


Figure 10. Frequency trend in the future scenario (2040) for the Reference Incident with primary regulation supported by FRUs.

The support provided by the FRUs improves both the dynamic and steady state frequency parameters. The frequency nadir is now $f_{nad} = 49.79$ Hz while the value at steady state is $\Delta f_{stat} = 49.84$ Hz. Even if there is some distance from the frequency parameters of the base scenario in 2020, the entrance of FRUs in the regulation chain leads to a safer and reliable management of the synchronous area.

4.3. Primary regulation with Fast Reserve Unit and additional Synthetic Inertia control in the 2040 Scenario

In this case, the SI control is assumed as an additional feature of the converters connecting the FRU to the grid. The inclusion of this control allows the system to be supported from the point of view of the inertia with an improvement in dynamic parameters as RoCoF and frequency nadir. Figure 11 shows the new control scheme: the SI control was implemented as part of the FRU scheme, whose input is the frequency deviation, while the output is the sum of the two power contribution limited by a saturator block that represents the maximum power of the converter.

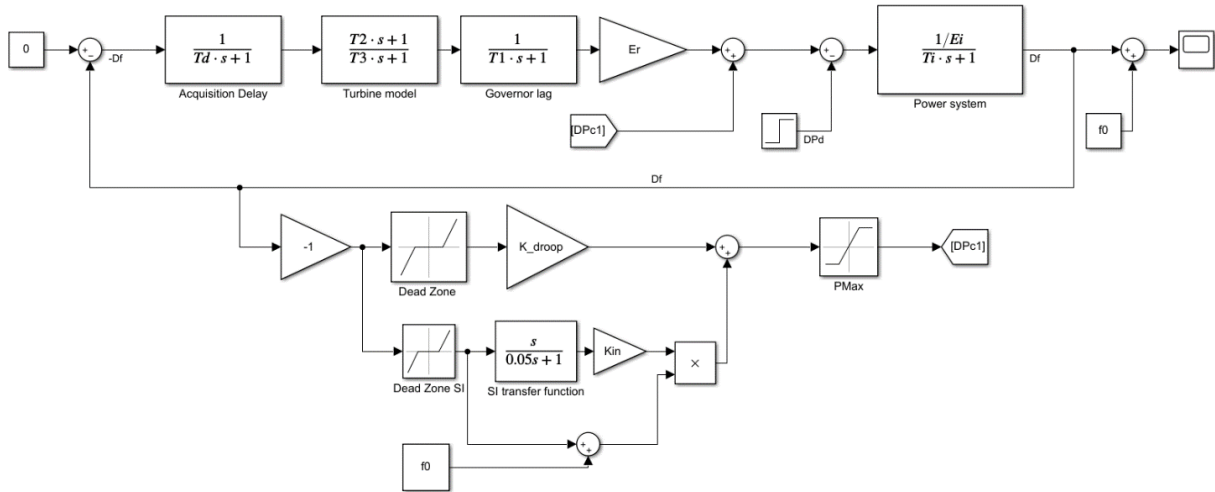


Figure 11. Implementation in Matlab/Simulink of the primary regulation control with FRUs and SI.

The frequency transient benefits from this implementation: the new frequency nadir is $f_{nad} = 49.80$ Hz. While the maximum Rocof remain unchanced due to the dead band that negate the regulation in the first moments of the unbalance, the slope of the curve is smoother than the previous case. Figure 12 shows the frequency trend in this last simulation and Figure 13 shows a detail of the transient in all the analyzed cases. Finally, Table 5 reports a summary of the frequency parameters retrieved from all the simulations.

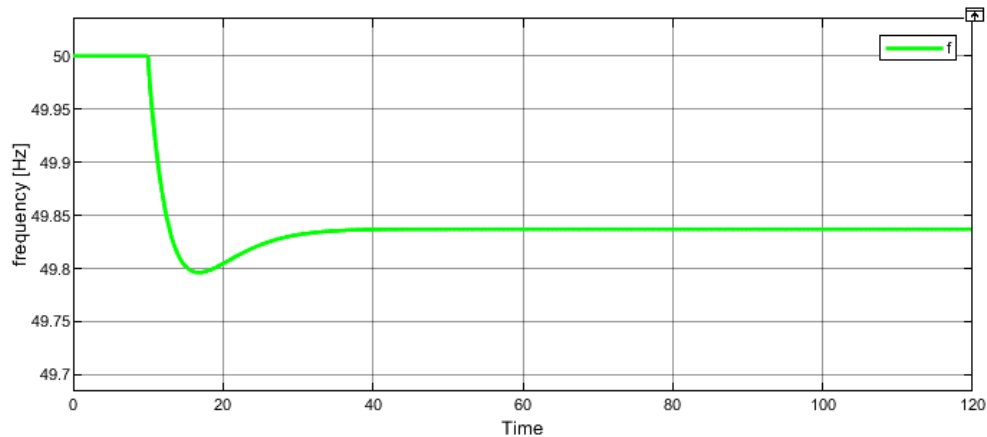


Figure 12. Frequency trend in the future scenario (2040) for the Reference Incident with primary regulation supported by FRUs and SI.

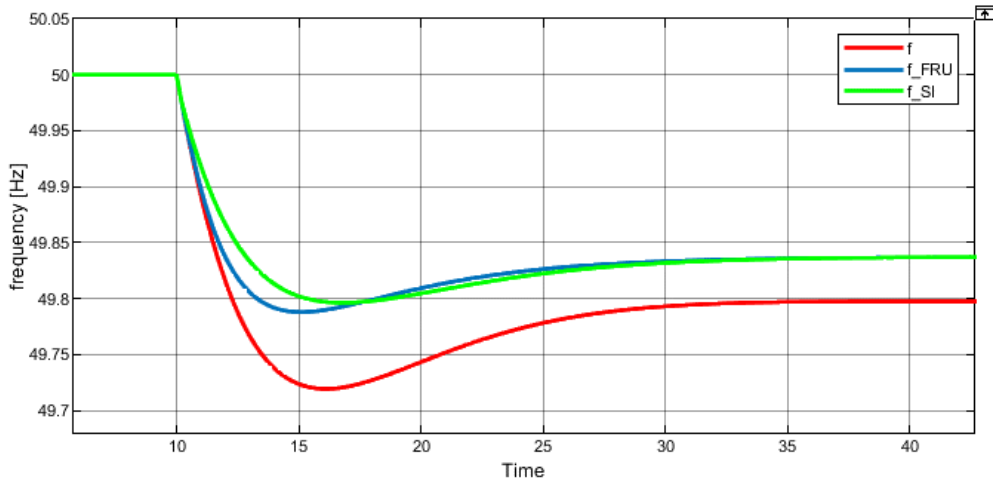


Figure 13. Frequency trends comparison in 2040 scenarios: traditional primary regulation (red line), primary regulation with FRU (blue line), primary regulation with combined FRU and SI (green line).

Table 5. Frequency parameters obtained from all the simulations.

Scenario	f_{nad} [Hz]	Δf_{stat} [Hz]	Rocof Hz/s
Base scenario 2020	49.87	49.91	-0.020
Future scenario 2040, traditional	49.72	49.79	-0.038
Future scenario 2040, FRU	49.79	49.84	-0.026
Future scenario 2040, FRU + SI	49.80	48.84	-0.022

5. Discussion

Some considerations are reported about the outcome of the presented study.

Firstly, it is worth discussing about the FRU total rated power. Simulations show that, under the hypotheses done in the previous sections, it is sufficient to activate about 4000 MW of FR to obtain in 2040 nearly the same steady-state error observed in 2020 for the reference incident of 3000 MW. FR is not the only solution for strengthening the power system and increasing its robustness to large disturbances but it is significant the fact that the required installed power is only 0.34% of the current total installed power in CE [34].

Following the same criteria established by the Italian FRU pilot project, the total power can be divided into between 160 and 800 installations with rated power between 5 MW and 25 MW, that can be easily connected both to MV and HV nodes of the power system without creating power flow issues difficult to solve. Figure 14 shows the solutions of connection of FRU with rated power below (a) and above 10 MW (b) elaborated according to the Italian technical standards [35]. PCC indicates the point of common coupling of the FRU with the grid, PCS indicates power conditioning systems (DC/AC converters) and EES indicates the Electric Energy Storage units.

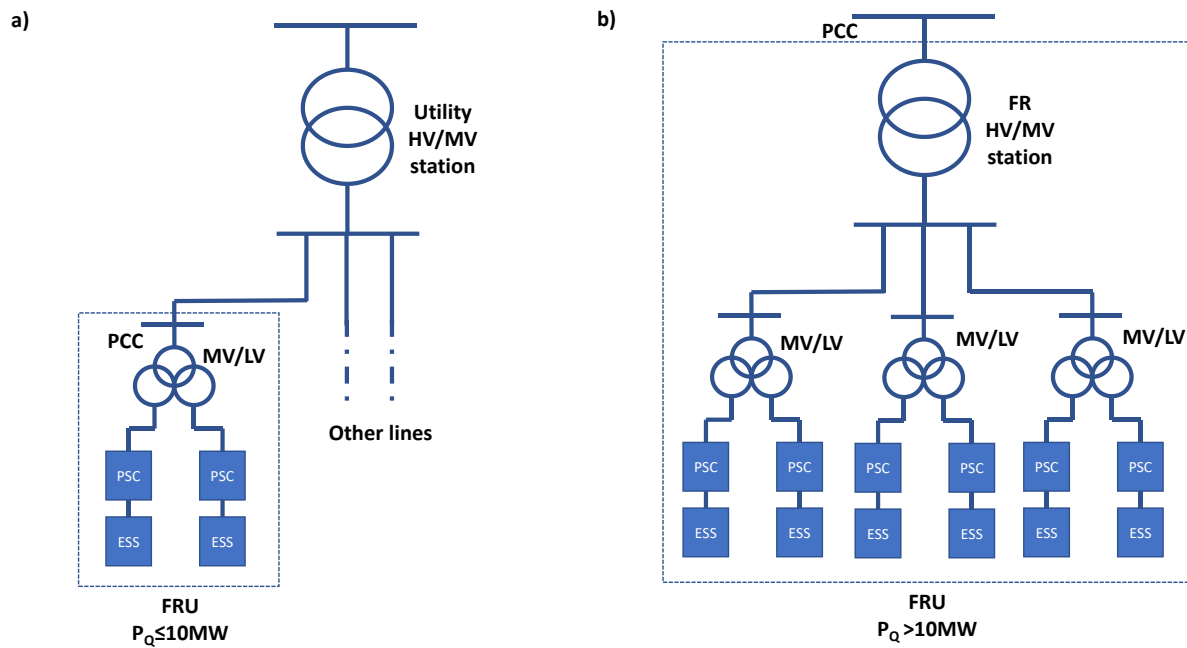


Figure 14. Connection of FRUs to the utility grid: a) rated power less or equal to 10 MW; b) rated power above 10 MW.

Moreover, the units could be independent plants or electric storage units associated with RES-based plants (hydro power plants, wind or PV plants, and so on [36-38]), normally managed for different purposes like energy arbitrage, peak shaving, etc. and locally controlled for providing the FR and SI services as soon as the frequency falls outside the dead band of the controller.

The territory occupation parameter for such installations, calculated according to the utility grid-size commercial Li-ion systems is about 8-13 kW/m² considering the area for auxiliary services, internal pathways and excluding the HV/MV station. Therefore, the search for free areas for installing FRUs close to HV/HV or HV/MV stations does not represent a serious issue for the diffusion of these systems.

How to divide the total rated power of the FRU calculated for the 2040 scenario among the CE countries? Two feasible criteria are suggested in this paper. The first one considers that the rated power to be installed in each country is proportional to the dismissed rated thermal capacity of that country, according to the proportion 20 MW of FRU per every 600 MW of thermal power.

A second criteria is to divide the total rated capacity according to the contribution factors of each country to the frequency containment reserve, calculated in [30] as indicated by European regulation [39-41]. In this case, the FRU rated power to be installed in each country evaluated on the production and consumption data in [33] is reported in the following Table 7.

Regarding the provision of the SI service by the same FRUs, it is worth noting that this service depends only by the implemented control. Therefore, the recourse to SI from FRU does not imply necessarily additional costs for such plants.

Table 7. FRU rated power to be installed in each country.

Country	Contribution factor	FRU rated power [MW]
Albania	0.26	11
Austria	2.55	104
Bosnia and Herzegovina	0.44	18
Belgium	3.04	123
Bulgaria	1.34	54
Switzerland	2.34	95
Czech Republic	2.37	96
Germany	17.49	710
Denmark	1.25	51
Spain	8.93	363
France	18.16	738
Greece	1.85	75
Croatia	0.66	27
Hungary	1.53	62
Italy	11.58	470
Luxembourg	0.25	10
Montenegro	0.12	5
North Macedonia	0.24	10
Netherlands	4.21	171
Poland	5.54	225
Portugal	1.81	74
Romania	2.09	85
Serbia	1.39	56
Slovenia	0.53	22
Slovakia	1.09	44
Turkey	8.91	362

The simulations so far conducted demonstrate that, with a minimum spread of FRUs in the CE grid, the reliability and the stability of the system are enhanced even in scenarios with a high penetration of inverter-based generation systems. Beside RES integration, FRUs contribution could be helpful on controlling frequency drifts in presence of extraordinary operating conditions of the grid. One of the most critical events that can occur on the electrical system is the separation in different frequency islands due to faults and malfunctions. This system split event can be, sometimes, more critical than the reference incident itself and, for this reason, it is interesting to analyze how FRUs or equivalent devices can support the grid during its occurrence. On January 8th, 2021, a tripping of a 400 kV busbar coupler in Croatian network caused a sequence of overcurrent that led to the split of CE system in two areas [42]. The countries of the CE system were divided as follows:

- Portugal, Spain, France, Italy, Switzerland, Luxembourg, Belgium, Netherlands, Germany, Denmark, Austria, Slovenia, Czech Republic, Poland, Slovakia and Hungary in the North-West area, with total load 317 GW, rated power of the generators 434 GVA, total power frequency characteristic 28.75 GW/Hz;
- Croatia, Romania, Bosnia Herzegovina, Serbia, Montenegro, North Macedonia, Albania, Bulgaria, Greece and Turkey in the South-East area, with total load 65 GW, rated power of the generators 89 GVA, total power frequency characteristic 5.89 GW/Hz.

The system split resulted in an equivalent deficit of power in the North-West area and an excess of power in the South-East area of approximately 6.3 GW. In order to assess the impact that the presence of FRUs in all the CE synchronous area would have had during the event, simulations have been carried out using the models presented in Section 4 and assuming the theoretical distribution of the FRUs reported in Table 7. The system parameters have been set according to the study in [**Errore. L'origine riferimento non è stata trovata.**]. According to the division of the CE countries into the two areas, the FRU qualified power was distributed as follows:

- Qualified Power of FRUs in North-West area: 3360 MW
- Qualified Power of FRUs in South-West area: 670 MW

Figure 16 shows the simulated frequency trends in the two areas following the split. As discussed in [**Errore. L'origine riferimento non è stata trovata.**], the differences with the real trends during the system split in January are due to not having implemented in simulation the action of the defense mechanisms that were activated during the split. Nevertheless, the steady-state values of the frequency and the timing of the frequency evolution in the two area are those really measured after the separation of the synchronous area. Figure 17 shows the frequency trends in the same system that would have occurred, under the same hypotheses, in presence of FRUs.

The contribution of the fast frequency regulation leads to lower steady-state deviations in both areas, confirming the effectiveness of this technology. Table 8 summarizes the steady-state values of the frequency. It is worth nothing that, although the SE area contains the lowest amount of fast reserve capacity, the effects of FRUs intervention on the frequency steady-state deviation and nadir is the most evident. This is due to the smaller power-frequency characteristic of the SE part with respect to the NW part. Indeed, the impact of the FRU will be higher in case of a relatively weak area with a low power-frequency characteristic given by traditional generators.

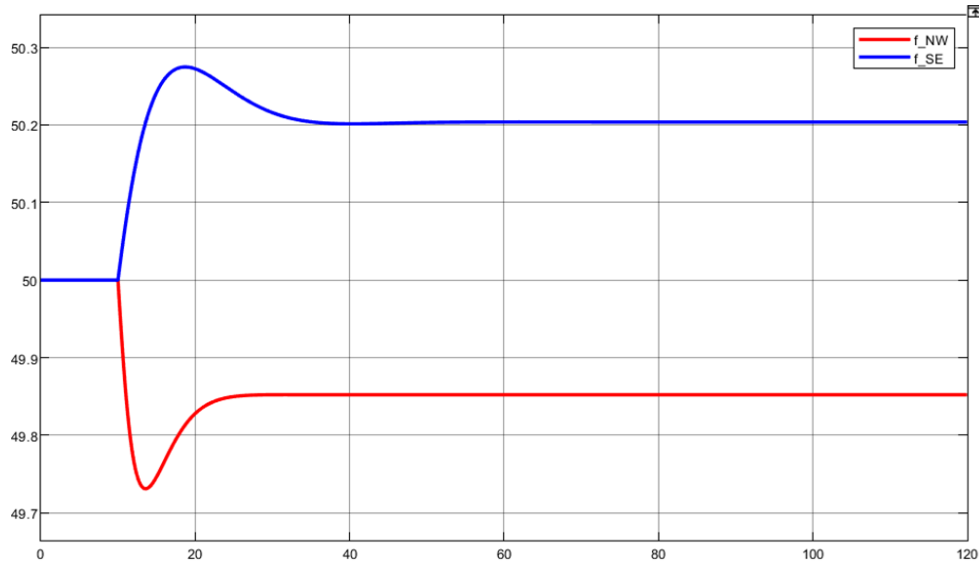


Figure 16. Frequency trends in the two areas after the split without FRUs.

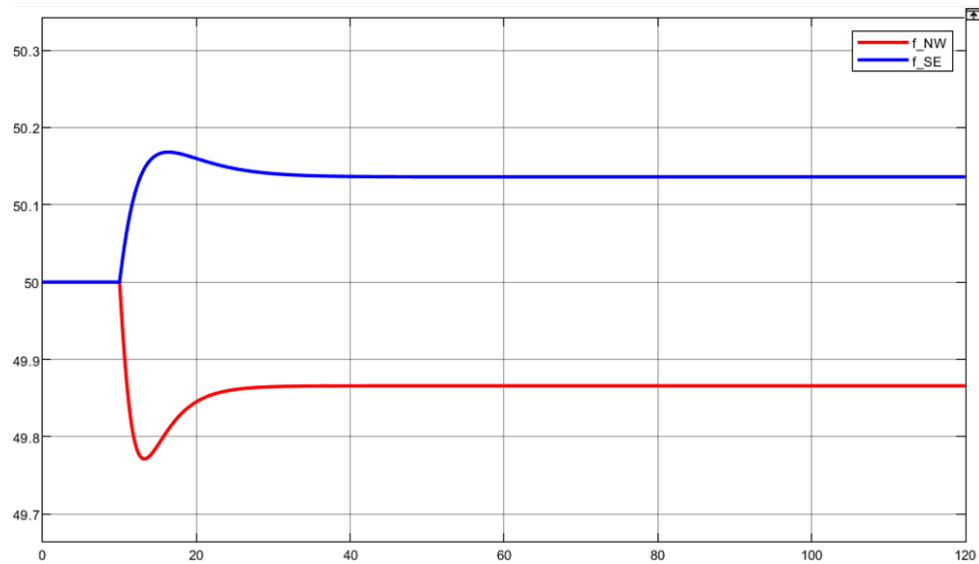


Figure 17. Frequency trends in the two areas after the split with FRUs.

Table 8. Frequency at steady-state after the split for the analyzed cases.

Scenario	Δf_{stat} [Hz]
NW Area without FRUs	49.85
SE Area without FRUs	50.20
NW Area with FRUs	49.87
SE Area with FRUs	50.13

7. Conclusions

The paper has presented the results of a simulation study on the application of battery storage systems in Fast Reserve Unit (FRU) configuration with an additional control for providing SI in the CE

synchronous area. For the European power system, studies and analysis concerning inertial response and frequency dynamics are particularly relevant, especially in sight of the events which can affect the stability and the safe operation of the system, as for instance the split occurred in January 2021 and the consequent severe frequency transients. The simulations, comparing the current scenario with a future (2040) scenario characterized by higher penetration of RES and lower inertia, have shown the advantages of the diffusion of FR in all Europe. In particular, the study demonstrates how 2040 frequency parameters can become comparable with the current ones with only 4000 MW of FRUs, showing the strategic importance of such a service in future electric power systems.

Finally, with this analysis, the authors want to underline the importance of investing in grid-scale storage for frequency support, especially at the sight of the reduction of the primary reserve that will occur in the next decades. Nevertheless, according to the last data from IEA, around the globe, 2.9 GW of storage capacity were added to electricity systems in 2019, that is almost 30% less than in 2018 [43]. The most of new storage systems are behind-the-meter installations instead of grid-scale storage systems. The factors behind this important reduction must be found in the uncertainty on two main aspects:

- the double charging of these systems in many Countries (partially solved with the Clean Energy Package);
- the possibility that Member States authorizes TSOs and DSOs to own and manage energy storage systems for grid support.

The results of this study show how much important for power systems' future will be to solve these problems in the shortest time.

References

1. G. Donnini, E. M. Carlini, G. Giannuzzi, R. Zaottini, C. Pisani, E. Chiodo, D. Lauria, F. Motola, On the Estimation of Power System Inertia accounting for Renewable Generation Penetration, 12th AEIT International Annual Conference, Italy, 23 September 2020.
2. L. Michi, M. Migliori, A. Caldarulo Bugliari, B. Aluisio, G. M. Giannuzzi, E. M. Carlini, Transmission network expansion planning: towards enhanced renewable integration, 2018 AEIT International Annual Conference, Bari (Italy), 3-5 Oct. 2018.
3. F. Parma, S. Pasquini, M. Pozzi, C. Bovo, M. Merlo, G. Giannuzzi, R. Zaottini, A tool to investigate the PV and storage plants effective integration in the European interconnected transmission network, 013 International Conference on Clean Electrical Power (ICCEP), Alghero (Italy), 11-13 June 2013.

4. ENTSO-E, Need for synthetic inertia (SI) for frequency regulation - ENTSO-E guidance document for national implementation for network codes on grid connection, **2017**.
5. Terna S.p.A., Piano di sviluppo della Rete di Trasmissione Nazionale, **2020**.
6. M. R. Rapizza, S. Canevese, Optimal Design for Synthetic Inertia and Fast Frequency Regulation in a Power System with High Penetration of Renewable Energy Sources, 2019 IEEE 15th International Conference on Control and Automation (ICCA), Edinburgh (UK), 16-19 July 2019.
7. Terna S.p.A., “Fast Reserve”, available at: <https://www.terna.it/en/electric-system/pilot-projects-pursuant-arera-resolution-300-2017-reel/fast-reserve-pilot-project>.
8. D. Fernandez-Muñoz, I. Guisandez, J. I. Perez-Diaz, M. Chazarra, A. Fernandez-Espina, F. Burke, “Fast Frequency Control Services in Europe”, 2018 15th International Conference on the European Energy Market (EEM), 27-29 June 2018, Lodz (Poland).
9. S. Canevese, D. Cirio, A. Gatti, M. Rapizza, E. Micolano, L. Pellegrino, “Simulation of Enhanced Frequency Response by Battery Storage Systems: the UK versus the Continental Europe System”, 2017 IEEE International Conference on Environment and Electrical Engineering and 2017 IEEE Industrial and Commercial Power Systems Europe (EEEIC / I&CPS Europe), 6-9 June 2017, Milan (Italy).
10. A. Mujcinagic, M. Kusljugic, E. Nukic, “Wind Inertial Response Based on the Center of Inertia Frequency of a Control Area”, *Energies* 2020, 13, 6177.
11. ENTSO-E. Initial Dynamic Model of Continental Europe. Available online: <https://docstore.entsoe.eu/publications/systemoperations-reports/continental-europe/Initial-Dynamic-Model/Pages/default.aspx> (accessed on April 2021).
12. M. Fiorelli, D. Keles, F. Montana, G. L. Restifo, E. Riva Sanseverino, G. Zizzo, “Evaluation of the Administrative Phase-Out of Coal Power Plants on the Italian Electricity Market”, *Energies*, **2020**, vol. 13, article 4596.
13. Terna S.p.A., “ALLEGATO 3: Requisiti tecnici dei dispositivi inclusi in Fast Reserve Unit”, **2019**.
14. ARERA, Deliberazione 200/20/R/EEL “Approvazione del regolamento predisposto da Terna s.p.a, ai sensi della deliberazione dell’Autorità 300/2017/R/EEL relativo al progetto pilota per l’erogazione del servizio di regolazione ultra-rapida di frequenza”, Italy, 03 June 2020.
15. Terna S.p.A, Stima delle ore di disponibilità per il servizio Fast Reserve per l’anno 2021, 06 Nov. 2020, available at: https://download.terna.it/terna/Stima%20Ore%20di%20Disponibilit%C3%A0%202021_8d8824de1d29fa4.pdf

16. Terna S.p.A, Progetto Pilota Fast Reserve – Esiti Asta, 10 Dec. 2020, available at: <https://www.terna.it/it/sistema-elettrico/pubblicazioni/news-operatori/dettaglio/esiti-asta-Fast-reserve>
17. Z. Jietang, Q. Linan, R. Pestana, L. Fengkui, Y. Libin, Dynamic frequency support by photovoltaic generation with synthetic inertia and frequency droop control, 2017 IEEE Conference on Energy Internet and Energy System Integration (EI2), Beijing (China), 26-28 Nov. 2017.
18. V. Knap, S. K. Chaudhary, D. L. Stroe, M. J. Swierczynski, B-I. Craciun, R. Teodorescu, Sizing of an Energy Storage System for Grid Inertial Response and Primary Frequency Reserve, *IEEE Transactions on Power Systems*, 2016, vol. 31(5), pp. 3447-3456.
19. P. Kundur, *Power System Stability and Control*, new edition, McGraw-Hill Education, New York, USA, 1994.
20. Tielens, P.; Hertem, D.V. The relevance of inertia in power systems. *Renew. Sustain. Energy Rev.* **2016**, *55*, 999–1009.
21. ENTSO-E, Inertia and Rate of Change of Frequency (RoCoF), Version 17, SDP-Inertia TF, Dec. 16 2020.
22. U. Tamrakar, D. Shrestha, M. Maharjan, B. P. Bhattarai, T. M. Hansen, R. Tonkoski, Virtual Inertia, Current Trends and Future Directions, *Applied Sciences*, **2017**, vol. 7, no. 7, p. 654.
23. Z. Jietang, Q. Linan, R. Pestana, L. Fengkui, Y. Libin, Dynamic frequency support by photovoltaic generation with synthetic inertia and frequency droop control, 2017 IEEE Conference on Energy Internet and Energy System Integration (EI2), Beijing (China), 26-28 Nov. 2017.
24. S. Canevese, A. Iaria and M. Rapizza, "Impact of fast primary regulation and synthetic inertia on grid frequency control," *2017 IEEE PES Innovative Smart Grid Technologies Conference Europe (ISGT-Europe)*, 2017, pp. 1-6.
25. V. Knap, S. K. Chaudhary, D. L. Stroe, M. J. Swierczynski, B-I. Craciun, R. Teodorescu, Sizing of an Energy Storage System for Grid Inertial Response and Primary Frequency Reserve, *IEEE Transactions on Power Systems*, 2016, vol. 31(5), pp. 3447-3456.
26. A. Semerow, S. Höhn, M. Luther, W. Sattinger, H. Abildgaard, A.D. Garcia, G.M. Giannuzzi, Dynamic Study Model for the Interconnected Power System of Continental Europe in Different Simulation Tools, in Proceedings of the *2015 IEEE Eindhoven, PowerTech*, Eindhoven, The Netherlands, 29 June–2 July 2015.
27. L. Busarello, R. Musca, Impact of high share of converter-interfaced generation on electromechanical oscillations in Continental Europe power system, *IET Renewable Power Generation*, **2021**.
28. F. Parma, S. Pasquini, M. Pozzi, C. Bovo, M. Merlo, G. Giannuzzi, R. Zaottini, A tool to investigate the PV and storage plants effective integration in the European interconnected transmis-

sion network, in Proceeding of the *2013 Int. Conf. on Clean Electrical Power (ICCEP)*, Alghero, Italy, 11–13 June 2013.

29. M. G. Ippolito, R. Musca, G. Zizzo, M. Bongiorno, Extension and Tuning of Virtual Synchronous Machine to Avoid Oscillatory Instability in Isolated Power Networks, 12th AEIT International Annual Conference, Italy, 23 September 2020.

30. M.G. Ippolito, R. Musca, G. Zizzo, Analysis and Simulations of the Primary Frequency Control during a System Split in Continental Europe Power System, *Energies*, **2021**, *14*, 1456.

31. ENTSO-E, Europe Power System 2040: completing the map & assessing the cost of non-grid, available at: <https://tyndp.entsoe.eu/tyndp2018/power-system-2040/>.

32. ENTSO-E, Completing the map - Power system needs, available at: <https://tyndp.entsoe.eu/system-needs/>.

33. ENTSO-E, Visualization Platform – Electricity Data, available at: <https://2020.entsos-tyndp-scenarios.eu/visualisation-platform-electricity-data/>.

34. ENTSO-E, Statistical Factsheet 2018, available at: <https://www.entsoe.eu/publications/statistics-and-data/#statistical-factsheet>.

35. CEI Standard 0.16, Reference technical rules for the connection of active and passive consumers to the HV and MV electrical networks of distribution Company, 2019.

36. F. Bignucolo, R. Caldon, M. Coppo, F. Pasut, M. Pettinà, Integration of Lithium-Ion Battery Storage Systems in Hydroelectric Plants for Supplying Primary Control Reserve, *Energies*, **2017**, *vol. 10*, no. 98.

37. M. Świerczyński, D. I. Stroe, A. Stan, R. Teodorescu, D. U. Sauer, Selection and Performance-Degradation Modeling of LiMO /Li Ti O and LiFePO /C Battery Cells as Suitable Energy Storage Systems for Grid Integration With Wind Power Plants: An Example for the Primary Frequency Regulation Service, *Ieee Transactions on Sustainable Energy*, **2014**, *vol. 5*, no. 1

38. M. Sandelic, D. I. Stroe, F. Iov, “Battery Storage-Based Frequency Containment Reserves in Large Wind Penetrated Scenarios: A Practical Approach to Sizing”, *Energies*, **2018**, *vol. 11*, article 3065.

39. ENTSO-E. Operation Handbook OpHB, Policy 1: Load-Frequency Control and Performance; Version 3.0; ENTSO-E: Brussels, Belgium, March 2009.

40. Commission Regulation (EU) 2017/2195 of 23 November 2017 establishing a guideline on electricity balancing.

41. ENTSO-E. All CE TSOs Proposal for the Dimensioning Rules for FCR in Accordance with Article 153(2) of the Commission Regulation (EU) 2017/1485 of 2 August 2017 Establishing a

Guideline on Electricity Transmission System Operation; ENTSO-E: Brussels, Belgium, August 2018.

42. ENTSO-E. System separation in the Continental Europe Synchronous Area on 8 January 2021—2nd update. Available online: <https://www.entsoe.eu/news/2021/01/26/system-separation-in-the-continental-europe-synchronous-area-on-8-january-2021-2nd-update/> (accessed on 02 June 2021).

43. International Energy Agency. Energy Storage. More efforts needed. June 2020. Available online: <https://www.iea.org/reports/energy-storage> (accessed on 02 June 2021).